An Efficient Reliability Analysis Method under Hybrid Uncertainty for High-Dimensional Problems

Zi-Xin Zhang, Pei-Pei Li*, and Yan-Gang Zhao
Department of Civil Engineering, Beijing University of Technology, Beijing 100124, China, S202489012@emails.bjut.edu.cn
Department of Civil Engineering, Beijing University of Technology, Beijing 100124, China, li.peipei@bjut.edu.cn
Department of Civil Engineering, Beijing University of Technology, Beijing 100124, China, zhaoyg@bjut.edu.cn

Abstract. In engineering reliability assessment, simultaneously considering hybrid uncertainty is crucial for ensuring structural safety and cost efficiency. Accurately characterizing the distribution of the conditional failure probability (CFP) is therefore of great practical importance. However, when the epistemic uncertainty involves high dimensional parameters, obtaining this distribution remains a significant challenge. To address this issue, this study proposes an efficient and accurate approach that integrates simulation-based post-processing with Bayesian inference to construct the CFP distribution. Parameter samples are first generated using a good lattice point method with partially stratified sampling, followed by reliability analysis to obtain CFP realizations. Beta mixture distribution model is then employed to directly fit the CFP, with Bayesian estimation used to determine the shape parameters of the mixture. The efficiency and accuracy of the proposed approach are demonstrated through two numerical examples, covering bimodal distributions and finite-element frame structures.

Keywords: Conditional failure probability; Probability distribution; High-dimensional; Beta mixture; Bayesian estimation

1. Introduction

In practical engineering, uncertainties are inevitable, arising from material variability, measurement errors, modeling simplifications, and external disturbances (Li et al., 2022a). Generally speaking, uncertainties can be divided into two types: aleatory uncertainty and epistemic uncertainty (Der Kiureghian and Ditlevsen, 2009). Aleatory uncertainty reflects the inherent randomness of physical variables and is irreducible, whereas epistemic uncertainty stems from limited knowledge and can be reduced with additional data or improved models. Traditional reliability analysis typically considers only aleatory uncertainty, which is modeled using random variables, leading to a deterministic failure probability. However, in real engineering applications, such as wind loads on bridges, limited data and measurements introduce significant epistemic uncertainty, making it difficult to establish

* Corresponding author

accurate probabilistic models. In other words, improved knowledge leads to more accurate modeling. As pointed out by Der Kiureghian and Ditlevsen (Der Kiureghian and Ditlevsen, 2009), neglecting the distinction between these two types of uncertainty may result in biased estimates of the failure probability. Therefore, structural reliability analysis under hybrid uncertainty is of great importance (Hoffman and Hammonds, 1994).

Currently, three main frameworks are used to model hybrid uncertainty: probability boxes (p-boxes) (Faes et al., 2021; Yang et al., 2023), fuzzy probability (Möller and Beer, 2013), and hierarchical probabilistic models (Zhao et al., 2018; Zhao and Lu, 2021; Chen and Wan, 2019). Among them, hierarchical probabilistic models have attracted considerable attention because they naturally incorporate Bayesian updating to reduce epistemic uncertainty (Li et al., 2025). This framework describes hybrid uncertainty using a two-level probabilistic structure, where epistemic and aleatory uncertainties are represented at the outer and inner levels, respectively. Within this framework, the failure probability becomes dependent on epistemic parameters and is thus treated as a random variable, referred to as the conditional failure probability (CFP). Accordingly, the conditional reliability index (CRI) is also uncertain (Kiureghian, 1989).

In practical applications, uncertainty in distribution parameters is often a dominant source of epistemic uncertainty and can significantly affect reliability assessment results. Various methods have been developed to account for this effect, including the first-order second-moment method (Zhao and Jiang, 1992), point-estimate methods (Hong, 1996), and first-order approximation methodology (Der Kiureghian, 2008), which aim to estimate the predictive failure probability (PFP). However, while PFP reflects the influence of parameter uncertainty, it cannot fully characterize the variability and distributional features of the CFP (Zhao et al., 2018).

Therefore, it is essential to characterize the probability distribution of the CFP for a more transparent assessment of structural risk. To this end, Ang and De Leon (Ang and De Leon, 2005) employed the Monte Carlo simulation (MCS) for estimating the expected and percentile values of the conditional probability of failure, but the method is computationally expensive to obtain a large number of CFP samples to ensure the accuracy of the results, especially for large- scale structures. Later, Der Kiureghian et al. (Der Kiureghian and Ditlevsen, 2009) derived the explicit PDF of CFP for the case of a linear limit-state function and normal random variables. For general cases, it is difficult to obtain the explicit PDF of CFP /CRI. Zhao et al. (Zhao et al., 2018) proposed a novel statistical analysis approach to determine the PFP and quantiles of CFP. However, the results of PFP may be unreliable when the variability of CFP is large. Li et al. (Li et al., 2022a; Li et al., 2022b) employed the first four/three moments of CRI and unimodal distribution (three-parameter normal/lognormal distribution) to fit the CRI distribution. However, this method may not accurately capture the characteristics of a bimodal CRI distribution in practical engineering, which would result in a loss of precision. Recently, Leng et al. (Leng et al., 2025) designed a fixed sampling distribution and used KDE to fit the CFP distribution. However, it is not suitable for high- dimensional or nonlinear problems, which limits its applicability in practical engineering applications.

To address these limitations, this study develops an efficient and robust method to directly approximate the distribution of the CFP under high-dimensional parameter uncertainty. A flexible bounded mixture of Beta distributions model is employed to accurately represent the CFP. The model parameters are efficiently estimated by combining advanced sampling strategies with

Bayesian inference. The remainder of this paper is organized as follows. In Section 2, the problem formulation considering parameter uncertainty is introduced. Section 3 introduces the proposed an efficient reliability analysis method under hybrid uncertainty for high-dimensional problems. Two numerical examples are studied in Section 4 to illustrate the proposed method. Section 5 concludes the paper with some final remarks.

2. Problem Formulation

Structural reliability analysis aims to evaluate the failure probability of a structure. The failure probability P_f is theoretically defined as

$$P_f = \int_{G(\boldsymbol{X})\leq 0} f_{\boldsymbol{X}}(\boldsymbol{x})\, d\boldsymbol{x} \tag{1}$$

where $\boldsymbol{X} = [X_1, X_2, ..., X_n]$ is an n-dimensional vector of independent random variables, representing uncertainties in material properties, geometric parameters, loads, and environmental conditions. Here, $f_{\boldsymbol{X}}(\boldsymbol{x})$ is the joint probability density function (PDF) of $\boldsymbol{X}$, and $G(\boldsymbol{X})$ is the performance function, with $G(\boldsymbol{X}) \leq 0$ defining the failure domain.

Eq. 1 represents the theoretical failure probability under perfect knowledge. However, in practical applications, available data are often limited or of low quality, leading to significant uncertainty in the estimation of distribution parameters (e.g., means and standard deviations). This introduces epistemic uncertainty into the reliability analysis.

In this study, the distribution parameter uncertainty is modeled by random variables notated as the vector $\boldsymbol{\Theta}$. Hence the failure probability becomes a random variable varying with $\boldsymbol{\Theta}$, denoted as $P_f(\boldsymbol{\Theta})$. It can be formulated as (Kiureghian, 1989):

$$P_f(\boldsymbol{\Theta}) = \int_{G(\boldsymbol{X})\leq 0} f_{X|\boldsymbol{\Theta}}(\boldsymbol{x}|\boldsymbol{\theta})\, d\boldsymbol{x} \tag{2}$$

where $f_{X|\boldsymbol{\Theta}}(\boldsymbol{x}|\boldsymbol{\theta})$ denotes the conditional joint PDF of random variables $\boldsymbol{X}$ based on the uncertain distribution parameters $\boldsymbol{\Theta}$.

To characterize the impact of parameter uncertainty, it is necessary to analyze the statistical properties of the CFP. However, evaluating Eq. 2 for different realizations of $\boldsymbol{\Theta}$ can be computationally demanding, especially for high-dimensional problems. Therefore, an efficient and robust approach is required for reliability assessment.

3. Proposed Method for High-Dimensional Reliability Analysis under Hybrid Uncertainty

This section presents a novel method for high-dimensional reliability analysis under hybrid uncertainty, based on a parameterized modeling approach for the conditional failure probability (CFP) combined with Bayesian inference. Section 3.1 introduces an efficient sampling strategy for generating distribution parameter samples. In Section 3.2, the PDF and CDF of the CFP are constructed explicitly using beta mixture model. Finally, Section 3.3 employs Bayesian inference to estimate the model parameters.

3.1. Generation of Conditional Failure Probability Samples

To improve sampling efficiency in high-dimensional parameter spaces, this study adopts the good lattice point method combined with partially stratified sampling (GLPM-PSS) proposed by Xu et al. (Xu and Dang, 2019). This approach integrates low-discrepancy sequences with partial stratified sampling (PSS) to maximize uniformity in high-dimensional sample spaces while reducing sample variance.

In GLPM-PSS, the high-dimensional space is first partitioned into several low-dimensional orthogonal subspaces using PSS, avoiding the infeasibility of full-dimensional stratification (Shields and Zhang, 2016). As shown in prior studies, significant variance reduction can be achieved when subspaces are one- or two-dimensional (Shields et al., 2015). Accordingly, for an even sample dimension s, the space is divided into $s/2$ two-dimensional subspaces, denoted as PSS - $2^{s/2}$; for odd s, it is divided into $(s-1)/2$ two-dimensional subspaces and one one-dimensional subspace, denoted as PSS - $2^{(s-1)/2} \times 1^1$. Uniform samples are straightforward in one-dimensional subspaces, while achieving uniformity in two-dimensional subspaces is crucial for overall variance reduction.

Among various low-discrepancy sequences such as Halton, GLPM, Sobol, and Hammersley, GLPM generates the most uniform two-dimensional point sets for a given sample size, thereby achieving maximum variance reduction. In practice, GLPM is applied to generate samples in the first two-dimensional subspace. Remaining two-dimensional subspaces are randomly permuted, and high-dimensional samples are assembled via random pairing. Finally, the inverse CDF transformation maps uniform high-dimensional samples into the physical space of the target parameters:

$$\theta^{(i)} = F_{\boldsymbol{\Theta}}^{-1}(u^{(i)}), \quad i = 1, 2, \ldots, N \tag{3}$$

where $u^{(i)}$ are samples from the uniform distribution on $[0, 1]$, N is the sample size, and $F_{\boldsymbol{\Theta}}^{-1}$ is the inverse CDF of the parameters $\boldsymbol{\Theta}$.

The high-dimensional parameter samples generated by GLPM-PSS are subsequently used in reliability analysis methods—such as the first-order reliability method (FORM), second-order reliability method (SORM), simulation-based approaches, high-order moment methods or surrogate models to obtain the corresponding CFP samples.

3.2. Selection of a Suitable Distribution Model for CFP

To obtain an accurate analytical expression of the CFP distribution, it is necessary to construct a parametric model with sufficient flexibility and adaptability. Common parametric models include the Pearson system (Pearson et al., 1979), Hermite model (Winterstein, 1988), saddle point approximation (Daniels, 1954), among others. However, these models often exhibit limited flexibility and are generally suited only for unimodal distributions, making them less effective in capturing complex multimodal or heavy-tailed behaviors.

Since the CFP is bounded between 0 and 1, the beta distribution naturally provides a suitable support. A single beta distribution with shape parameters α and β has the PDF:

$$f(X;\alpha,\beta) = \frac{\Gamma(\alpha+\beta)}{\Gamma(\alpha)\Gamma(\beta)}\, X^{\alpha-1}(1-X)^{\beta-1}, \quad 0 \le X \le 1, \tag{4}$$

and the corresponding CDF is

$$F(X;\alpha,\beta) = \int_0^x f(t;\alpha,\beta)\,dt \tag{5}$$

where $\Gamma(\cdot)$ is the Gamma function. By adjusting α and β, the beta distribution can represent a wide variety of shapes, including symmetric, left- or right-skewed, U-shaped, or bell-shaped distributions.

However, in practice, CFP distributions can exhibit long tails or even multimodal behavior, which a single beta distribution cannot fully capture. To accommodate these features, a beta mixture distribution with K components is adopted. Its PDF is expressed as

$$f_{P_f}(p) = \sum_{k=1}^{K} w_k\, f(p;\alpha_k,\beta_k), \quad 0 \le p \le 1, \tag{6}$$

where w_k denotes the weight of the k-th component $\sum_{k=1}^{K} w_k = 1$, K is the number of mixture components, and α_k, β_k are the shape parameters of that component. The corresponding CDF is given by

$$F_{P_f}(p) = \sum_{k=1}^{K} w_k\, F(p;\alpha_k,\beta_k). \tag{7}$$

The mean of the beta mixture distribution is given by

$$\mathbb{E}[P_f] = \sum_{k=1}^{K} w_k\, \frac{\alpha_k}{\alpha_k+\beta_k}, \tag{8}$$

and its variance can be computed as

$$\mathrm{Var}[P_f] = \sum_{k=1}^{K} w_k \frac{\alpha_k\beta_k}{(\alpha_k+\beta_k)^2(\alpha_k+\beta_k+1)} + \sum_{k=1}^{K} w_k \left(\frac{\alpha_k}{\alpha_k+\beta_k}\right)^2 - \mathrm{E}[P_f]^2. \tag{9}$$

The beta mixture model provides a flexible and explicit representation of the CFP distribution, capable of capturing skewness, heavy tails, and multimodality. This explicit representation facilitates subsequent risk quantification and reliability analysis.

3.3. Bayesian Estimation of Beta Mixture Model Parameters

In this study, a beta mixture distribution with two components is adopted to model the CFP, achieving a balance between flexibility and computational efficiency. For high-dimensional problems, traditional moment-based methods often require a large number of samples, which can be computationally expensive. In contrast, Bayesian estimation provides robust and reliable parameter estimates even with a limited number of samples, by combining prior knowledge with observed sample data.

To improve estimation stability, Bayesian inference is adopted, treating the shape parameters as random variables. For the two-component beta mixture distribution, the four shape parameters are denoted as $\boldsymbol{\phi} = (\alpha_1, \beta_1, \alpha_2, \beta_2)$ and a non-informative prior is assigned:

$$\pi_0(\boldsymbol{\phi}) \propto 1, \quad \alpha_1, \beta_1, \alpha_2, \beta_2 > 0. \tag{10}$$

To simplify the estimation and reduce the parameter dimension, the mixture weight of the first component is fixed at $w_1 = 0.7$, and the weight of the second component is determined as $w_2 = 1 - w_1$. This allows stable estimation of the shape parameters while maintaining the flexibility of the beta mixture model.

Let $\{p_i\}_{i=1}^{N}$ denote the CFP samples generated using the GLPM-PSS sampling method (Section 3.1) combined with reliability analysis techniques. The likelihood function for the beta mixture model is

$$L(\{p_i\} \mid \boldsymbol{\phi}) = \prod_{i=1}^{N} f_{P_f}(p_i \mid \boldsymbol{\phi}), \tag{11}$$

where $f_{P_f}(\cdot \mid \boldsymbol{\phi})$ is the PDF of the beta mixture distribution Eq. 6.

According to Bayes' theorem, the posterior distribution of the shape parameters is

$$\pi(\boldsymbol{\phi} \mid \{p_i\}) = \frac{L(\{p_i\} \mid \boldsymbol{\phi})\, \pi_0(\boldsymbol{\phi})}{\int L(\{p_i\} \mid \boldsymbol{\phi})\, \pi_0(\boldsymbol{\phi})\, d\boldsymbol{\phi}}. \tag{12}$$

The Bayesian estimate of the parameters is typically taken as the posterior mean:

$$\hat{\boldsymbol{\phi}} = \mathbb{E}[\boldsymbol{\phi} \mid \{p_i\}] = \int \boldsymbol{\phi}\, \pi(\boldsymbol{\phi} \mid \{p_i\})\, d\boldsymbol{\phi}. \tag{13}$$

Since this integral is generally intractable analytically, Markov Chain Monte Carlo (MCMC) methods Gibbs sampling (Geman and Geman, 1984; Zhao et al., 2025) is employed to generate posterior samples. The posterior mean is then approximated by the sample average:

$$\hat{\boldsymbol{\phi}} \approx \frac{1}{N_G} \sum_{i=1}^{N_G} \boldsymbol{\phi}^{(i)}, \tag{14}$$

where N_G is the total number of posterior samples, and $\boldsymbol{\phi}^{(i)}$ is the i-th sample.

This Bayesian estimation framework with fixed mixture weight ensures stable and reliable determination of the beta nixture shape parameters, even when the number of CFP samples is limited. With the estimated parameters, the beta mixture model can be used for CFP distribution representation and high-dimensional reliability analysis.

4. Numerical examples

4.1. Example 1: bimodal distributions

In this example, the performance function is considered:

$$G(\boldsymbol{X}) = 30\sqrt{2} + \sum_{i=1}^{200} X_i - 165 \tag{15}$$

The random variables are assumed to be mutually independent, and each variable follows a normal distribution with an unknown mean and unit standard deviation. The means are modeled using a Gaussian mixture distribution with two components (means of -10 and -3, standard deviations of 0.5, and weights of 0.7 and 0.3), while the remaining variables have means equal to 1 and variance 0.1.

Since $G(\boldsymbol{X})$ isa linear combination of independent normal random variables, the resulting response Z also follows a normal distribution. Its mean and variance can be explicitly obtained as $\mu_Z = a\sqrt{d} + \sum_{i=1}^{d} \mu_{X_i} - 165$, $\sigma_Z = \sqrt{\sum_{i=1}^{d} \sigma_i^2} = \sqrt{d}$. Accordingly, the reliability index and the failure probability can be expressed as

$$\beta = \frac{\mu_Z}{\sigma_Z} = \frac{a\sqrt{d} + \sum_{i=1}^{d} \mu_{X_i} - 165}{\sqrt{d}} \tag{16}$$

$$P_f = \Phi(-\beta) \tag{17}$$

where $\Phi(\cdot)$ denotes the CDF of the standard normal distribution.

For each realization of the mean vector, the failure probability is evaluated using Eqs. 16 and 17, yielding samples of the CFP. Based on these CFP samples, the proposed method is then employed to estimate the distribution of the failure probability. Fig. 1 illustrates the estimated PDF and CDF of the CFP based on 20 independent runs, together with the results obtained by the FSD-KDE approach and the reference solution from MCS with 10^8 samples. The results show that the proposed method is able to reproduce the bimodal nature of the CFP distribution more effectively than FSD-KDE. In particular, the estimated PDF aligns well with the MCS histogram, accurately capturing the locations of the peaks, while the corresponding CDF closely follows the empirical curve obtained from MCS. Furthermore, the PDFs obtained from repeated runs exhibit only minor variability, and the CDFs are nearly indistinguishable, indicating good stability and consistency of the proposed method.

Table I summarizes the mean, standard deviation, and the 0.75 and 0.90 quantiles of the CFP estimated by the proposed method and FSD-KDE, in comparison with the MCS results. It can be observed that the proposed method yields relative errors generally below 5%, demonstrating

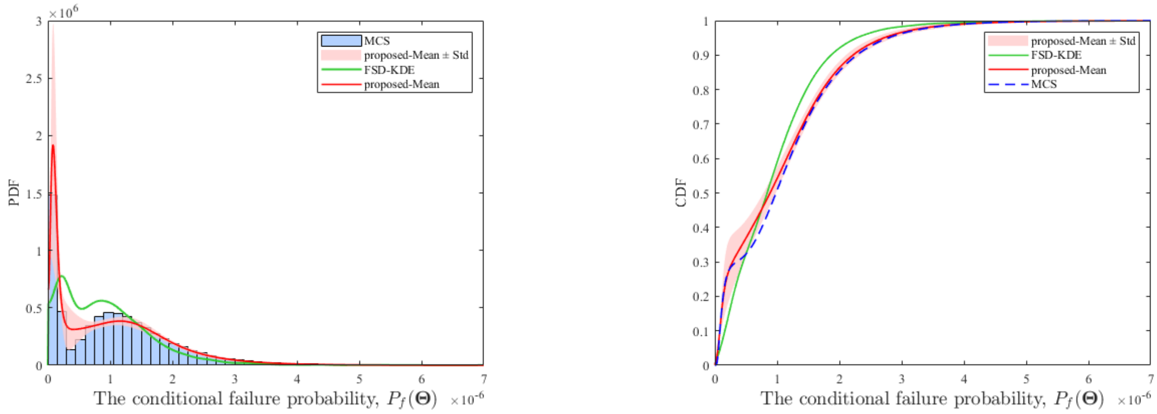

(a) PDF (b) CDF

Figure 1. Histogram with PDF and CDF of $P_f(\boldsymbol{\Theta})$ in Example 1.

Table I. Summary of some statistical values of CFP in Example 1.

Method	Mean of $P_f(\boldsymbol{\Theta})$	Std of $P_f(\boldsymbol{\Theta})$	75% quantile of $P_f(\boldsymbol{\Theta})$	90% quantile of $P_f(\boldsymbol{\Theta})$	N
MCS	1.086×10^{-6}	9.311×10^{-7}	1.594×10^{-6}	2.280×10^{-6}	10^8
The proposed method	1.069×10^{-6}	9.135×10^{-7}	1.613×10^{-6}	2.268×10^{-6}	377
	(1.565%, 0.026)	(1.890%, 0.039)	(1.192%, 0.035)	(0.526%, 0.038)	
FSD-KDE (Leng et al., 2025)	9.521×10^{-7}	7.410×10^{-7}	1.330×10^{-6}	1.855×10^{-6}	10^4
	(12.330%)	(20.417%)	(16.562%)	(18.640%)	
Zhao et al. (Zhao et al., 2018)	-	-	-	-	-

Note: Std denotes the standard deviation of the CFP, and N is the number of CFP samples. The the proposed method results are averaged over 20 independent runs. Values in parentheses denote the mean relative error with respect to MCS and the corresponding coefficient of variation (CoV).

improved accuracy over FSD-KDE. In addition, the corresponding coefficients of variation (CoV) remain at a low level, further confirming the robustness of the proposed method in handling bimodal distributions. It is also noted that the method proposed in Ref. (Zhao et al., 2018) is not applicable in this case due to its inability to capture bimodal behavior.

4.2. Example 2: A finite-element frame structure

The second example considers a five-story three-span portal steel frame structure subjected to lateral loads, as shown in Fig. 2, and has been studied in previous work (Blatman and Sudret, 2010; Wei and Rahman, 2007). Here, 21 random variables are defined as follows:

$$\boldsymbol{X} = [P_1, P_2, P_3, E_1, E_2, I_1, I_2, I_3, I_4, I_5, I_6, I_7, I_8, A_1, A_2, A_3, A_4, A_5, A_6, A_7, A_8] \tag{18}$$

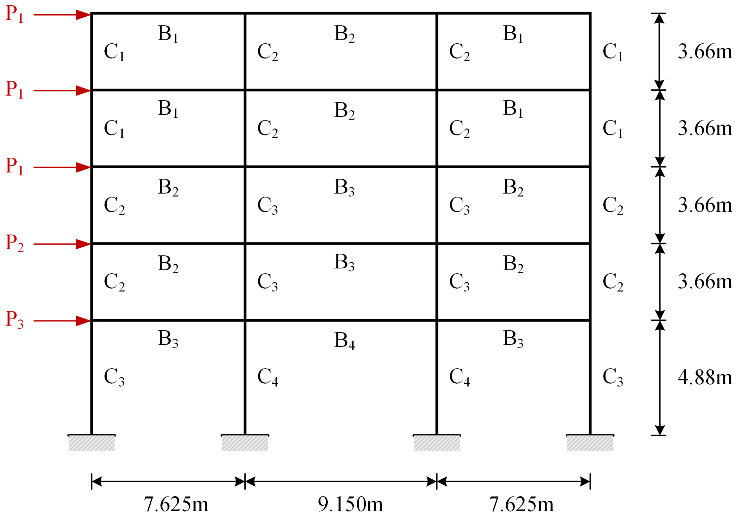

Figure 2. Five-story three-span frame

Table II. Properties of the frame element.

Element	Young's Modulus	Inertia moment	Cross-section area
B_1	E_1	I_5	A_5
B_2	E_1	I_6	A_6
B_3	E_1	I_7	A_7
B_4	E_1	I_8	A_8
C_1	E_2	I_1	A_1
C_2	E_2	I_2	A_2
C_3	E_2	I_3	A_3
C_4	E_2	I_4	A_4

These variables in the formula are assumed to be mutually independent. Since incomplete knowledge of the distributions of random variables is common in practical engineering, this example further accounts for distribution parameter uncertainty, in which both the means and standard deviations of the random variables are treated as random variables. The structural data and random variables statistical properties are shown in Tables II and III, respectively. In this study, for practical considerations, the lateral load is assumed to follow a lognormal distribution, whereas the material properties are modeled using a truncated normal distribution over the range $(0, +\infty)$ as suggested by Blatman and Sudret (Blatman and Sudret, 2010), as negative values for material properties are meaningless.

Similarly, 377 samples of the distribution parameters were generated using GLPM-PSS, and the corresponding 377 CFP samples were obtained via Subset Simulation. Based on the proposed

Table III. Distribution statistical characteristics of the random variables in Example 2.

Parameters	Distribution	Mean Value	Standard Deviation
P_1 (kN)	Lognormal	LN(133.454, 6.673)	LN(40.040, 2.002)
P_2 (kN)	Lognormal	LN(88.970, 4.449)	LN(35.590, 1.780)
P_3 (kN)	Lognormal	LN(71.175, 3.559)	LN(28.470, 1.424)
E_1 (kN/m^2)	Truncated normal $(0, +\infty)$	LN(2.174$\times 10^7$, 1.087$\times 10^6$)	LN(1.915$\times 10^7$, 9.576$\times 10^4$)
E_2 (kN/m^2)	Truncated normal $(0, +\infty)$	LN(2.380$\times 10^7$, 1.190$\times 10^6$)	LN(1.915$\times 10^7$, 9.576$\times 10^4$)
I_1 (m^4)	Truncated normal $(0, +\infty)$	LN(0.008, 4.050$\times 10^{-4}$)	LN(0.001, 5.500$\times 10^{-5}$)
I_2 (m^4)	Truncated normal $(0, +\infty)$	LN(0.012, 5.750$\times 10^{-4}$)	LN(0.001, 6.500$\times 10^{-5}$)
I_3 (m^4)	Truncated normal $(0, +\infty)$	LN(0.021, 1.100$\times 10^{-3}$)	LN(0.003, 1.300$\times 10^{-4}$)
I_4 (m^4)	Truncated normal $(0, +\infty)$	LN(0.026, 1.300$\times 10^{-3}$)	LN(0.003, 1.500$\times 10^{-4}$)
I_5 (m^4)	Truncated normal $(0, +\infty)$	LN(0.011, 5.400$\times 10^{-4}$)	LN(0.003, 1.300$\times 10^{-4}$)
I_6 (m^4)	Truncated normal $(0, +\infty)$	LN(0.014, 7.050$\times 10^{-4}$)	LN(0.004, 1.500$\times 10^{-4}$)
I_7 (m^4)	Truncated normal $(0, +\infty)$	LN(0.023, 1.200$\times 10^{-3}$)	LN(0.006, 2.800$\times 10^{-4}$)
I_8 (m^4)	Truncated normal $(0, +\infty)$	LN(0.026, 1.300$\times 10^{-3}$)	LN(0.007, 3.250$\times 10^{-4}$)
A_1 (m^2)	Truncated normal $(0, +\infty)$	LN(0.313, 1.565$\times 10^{-2}$)	LN(0.056, 2.800$\times 10^{-3}$)
A_2 (m^2)	Truncated normal $(0, +\infty)$	LN(0.372, 1.860$\times 10^{-2}$)	LN(0.074, 3.700$\times 10^{-3}$)
A_3 (m^2)	Truncated normal $(0, +\infty)$	LN(0.506, 2.530$\times 10^{-2}$)	LN(0.093, 4.700$\times 10^{-3}$)
A_4 (m^2)	Truncated normal $(0, +\infty)$	LN(0.558, 2.790$\times 10^{-2}$)	LN(0.112, 5.600$\times 10^{-3}$)
A_5 (m^2)	Truncated normal $(0, +\infty)$	LN(0.253, 1.270$\times 10^{-2}$)	LN(0.093, 4.700$\times 10^{-3}$)
A_6 (m^2)	Truncated normal $(0, +\infty)$	LN(0.291, 1.460$\times 10^{-2}$)	LN(0.102, 5.100$\times 10^{-3}$)
A_7 (m^2)	Truncated normal $(0, +\infty)$	LN(0.373, 1.870$\times 10^{-2}$)	LN(0.121, 6.000$\times 10^{-3}$)
A_8 (m^2)	Truncated normal $(0, +\infty)$	LN(0.419, 2.090$\times 10^{-2}$)	LN(0.195, 9.800$\times 10^{-3}$)

method, the PDF and CDF of the CFP were then constructed. Fig. 3 compares the histogram and empirical CDF obtained from 10^5 MCS samples with the results estimated by the proposed method and FSD-KDE. It can be observed that both the proposed method and FSD-KDE provide good agreement with MCS and successfully capture the main characteristics of the CFP distribution. In contrast, the method in Ref. (Zhao et al., 2018) only estimates the conditional reliability index and therefore does not directly provide the full distribution of CFP for comparison.

Table IV further summarizes the mean, standard deviation, and the 75% and 90% quantiles of the CFP obtained by different methods. The results indicate that the proposed method and FSD-KDE achieve relative errors within approximately 10%, while noticeable discrepancies are observed for the method of Zhao et al. (Zhao et al., 2018).

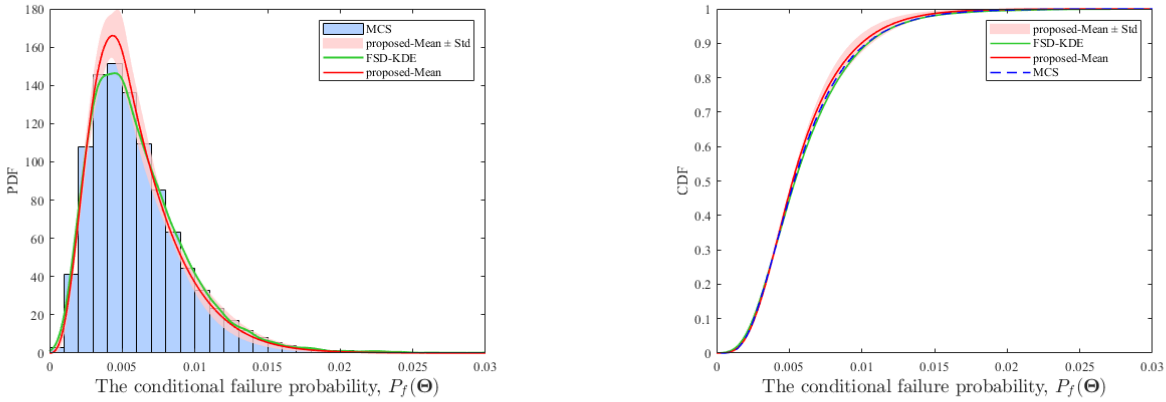

(a) PDF (b) CDF

Figure 3. Histogram with PDF and CDF of $P_f(\boldsymbol{\Theta})$ in Example 2.

Table IV. Summary of some statistical values of CFP in Example 2.

Method	Mean of $P_f(\boldsymbol{\Theta})$	Std of $P_f(\boldsymbol{\Theta})$	75% quantile of $P_f(\boldsymbol{\Theta})$	90% quantile of $P_f(\boldsymbol{\Theta})$	N
MCS	6.025×10^{-3}	3.292×10^{-3}	7.610×10^{-3}	1.034×10^{-2}	10^5
the proposed method	5.869×10^{-3}	3.051×10^{-3}	7.428×10^{-3}	9.977×10^{-3}	377
	(2.589%, 0.035)	(7.321%, 0.110)	(2.392%, 0.044)	(3.511%, 0.070)	
FSD-KDE (Leng et al., 2025)	6.078×10^{-3}	3.379×10^{-3}	7.739×10^{-3}	1.040×10^{-2}	10^4
	(0.880%)	(2.643%)	(1.695%)	(0.580%)	
Zhao et al. (Zhao et al., 2018)	2.559×10^{-3}	1.700×10^{-3}	3.325×10^{-3}	4.736×10^{-3}	42484

5. Concluding Remarks

This paper develops an efficient and robust approach for high-dimensional reliability analysis under hybrid uncertainty. The proposed method directly fits the CFP distribution and explicitly constructs its PDF and CDF, which facilitates risk quantification and reliability evaluation.

Numerical results show that the proposed method maintains accuracy comparable to the classic Monte Carlo simulation (MCS), but only needs a very small number of CFP samples. The scheme greatly reduces the computational burden.

Bayesian inference is used to estimate parameters of the beta mixture model. Combined with beta mixture modeling, the method can effectively capture complex CFP characteristics such as multimodality and skewness, which widely exist in practical engineering problems.

Moreover, the proposed method exhibits broad applicability under high-dimensional parameter uncertainty. It performs effectively for the tested cases, including bimodal CFP distributions and finite-element frame structures with high-dimensional parameter uncertainty.

Despite the above merits, the required number of CFP samples may increase considerably for ultra-high-dimensional problems with thousands of dimensions. In addition, the current framework adopts a two-level sampling scheme, resulting in relatively high computational overhead. Future research will focus on decoupling the nested computational structure to further improve computational efficiency.

Acknowledgements

The authors gratefully acknowledge the support of the National Key R&D Program of China (2023YFC3009300, 2023YFC3009302).

References

Ang, A.-S. and D. De Leon: 2005, 'Modeling and analysis of uncertainties for risk-informed decisions in infrastructures engineering'. *Structure and Infrastructure Engineering* **1**(1), 19–31.

Blatman, G. and B. Sudret: 2010, 'An adaptive algorithm to build up sparse polynomial chaos expansions for stochastic finite element analysis'. *Probabilistic Engineering Mechanics* **25**(2), 183–197.

Chen, J. and Z. Wan: 2019, 'A compatible probabilistic framework for quantification of simultaneous aleatory and epistemic uncertainty of basic parameters of structures by synthesizing the change of measure and change of random variables'. *Structural Safety* **78**, 76–87.

Daniels, H. E.: 1954, 'Saddlepoint approximations in statistics'. *The Annals of Mathematical Statistics* pp. 631–650.

Der Kiureghian, A.: 2008, 'Analysis of structural reliability under parameter uncertainties'. *Probabilistic Engineering Mechanics* **23**(4), 351–358.

Der Kiureghian, A. and O. Ditlevsen: 2009, 'Aleatory or epistemic? Does it matter?'. *Structural Safety* **31**(2), 105–112.

Faes, M. G., M. Daub, S. Marelli, E. Patelli, and M. Beer: 2021, 'Engineering analysis with probability boxes: A review on computational methods'. *Structural Safety* **93**, 102092.

Geman, S. and D. Geman: 1984, 'Stochastic relaxation, Gibbs distributions, and the Bayesian restoration of images'. *IEEE Transactions on pattern analysis and machine intelligence* **PAMI-6**(6), 721–741.

Hoffman, F. O. and J. S. Hammonds: 1994, 'Propagation of uncertainty in risk assessments: the need to distinguish between uncertainty due to lack of knowledge and uncertainty due to variability'. *Risk analysis* **14**(5), 707–712.

Hong, H.-P.: 1996, 'Evaluation of the probability of failure with uncertain distribution parameters'. *Civil Engineering Systems* **13**(2), 157–168.

Kiureghian, A. D.: 1989, 'Measures of structural safety under imperfect states of knowledge'. *Journal of Structural Engineering* **115**(5), 1119–1140.

Leng, Y., Y.-H. Fei, Y.-B. Jiang, L. Wang, and C.-H. Cai: 2025, 'Fixed sampling distribution determination method for structural reliability assessment with parameter uncertainty'. *Applied Mathematical Modelling* p. 116191.

Li, P.-P., Z.-H. Lu, and Y.-G. Zhao: 2022a, 'An effective and efficient method for structural reliability considering the distributional parametric uncertainty'. *Applied Mathematical Modelling* **106**, 507–523.

Li, P.-P., M. A. Valdebenito, C. Dang, M. Beer, and M. G. Faes: 2025, 'Aleatory and epistemic uncertainty in reliability analysis: An engineering perspective'. *Structural Safety* p. 102666.

Li, P.-P., Y.-G. Zhao, and Z. Zhao: 2022b, 'Efficient method for fully quantifying the uncertainty of failure probability'. *Computer Methods in Applied Mechanics and Engineering* **399**, 115345.

Möller, B. and M. Beer: 2013, *Fuzzy randomness: uncertainty in civil engineering and computational mechanics*. Springer Science & Business Media.

Pearson, E. S., N. L. Johnson, and I. W. Burr: 1979, 'Comparisons of the Percentage Points of Distributions with the Same First Four Moments, Chosen from Eight Different Systems of Frequency Curves'. *Communications in Statistics-Simulation and Computation* **8**(3), 191–229.

Shields, M. D., K. Teferra, A. Hapij, and R. P. Daddazio: 2015, 'Refined stratified sampling for efficient Monte Carlo based uncertainty quantification'. *Reliability Engineering & System Safety* **142**, 310–325.

Shields, M. D. and J. Zhang: 2016, 'The generalization of Latin hypercube sampling'. *Reliability Engineering & System Safety* **148**, 96–108.

Wei, D. and S. Rahman: 2007, 'Structural reliability analysis by univariate decomposition and numerical integration'. *Probabilistic Engineering Mechanics* **22**(1), 27–38.

Winterstein, S. R.: 1988, 'Nonlinear vibration models for extremes and fatigue'. *Journal of Engineering Mechanics* **114**(10), 1772–1790.

Xu, J. and C. Dang: 2019, 'A novel fractional moments-based maximum entropy method for high-dimensional reliability analysis'. *Applied Mathematical Modelling* **75**, 749–768.

Yang, L.-C., C.-X. Wang, C.-Y. Ling, and M. Xie: 2023, 'Reliability evaluation of an imprecise multistate system with mixed uncertainty'. *IEEE Transactions on Reliability* **73**(1), 478–491.

Zhao, Y.-G. and J.-R. Jiang: 1992, 'An Advanced First Order Second Monment Method'. *Earthquake Engineering and Engineering Vibration* **12**(4), 49–57. in Chinese.

Zhao, Y.-G., P.-P. Li, and Z.-H. Lu: 2018, 'Efficient evaluation of structural reliability under imperfect knowledge about probability distributions'. *Reliability Engineering & System Safety* **175**, 160–170.

Zhao, Y.-G., Y.-T. Liu, P.-P. Li, Y.-Y. Weng, M. A. Valdebenito, and M. G. Faes: 2025, 'A Bayesian piecewise fitting method for estimating probability distributions of performance functions'. *Reliability Engineering & System Safety* p. 111266.

Zhao, Y.-G. and Z.-H. Lu: 2021, *Structural reliability: approaches from perspectives of statistical moments*. John Wiley & Sons.